On the use of drift ice thickness statistics from a Copernicus reanalysis product for fatigue damage calculation

Hornnes, Vegard; Hammer, T.C.; Høyland, Knut V.; Hendrikse, H.; Turner, Joshua

Publication date
2022

Document Version
Final published version

Published in
Proceedings of the 26th IAHR International Symposium on Ice

IAHR AIRH

26th IAHR International Symposium on Ice

Montréal, Canada – 19-23 June 2022

On the use of drift ice thickness statistics from a Copernicus reanalysis product for fatigue damage calculation

Vegard Hornnes[1], Tim C. Hammer[2,3], Knut Vilhelm Høyland[1], Hayo Hendrikse[2], Joshua Turner[4]

[1] Department of Civil and Environmental Engineering, Norwegian University of Science and Technology,
Høgskoleringen 7A, 7491 Trondheim, Norway
vegard.hornnes@ntnu.no
[2] Delft University of Technology, Delft, The Netherlands
[3] Siemens Gamesa Renewable Energy, The Hague, The Netherlands
[4] Carleton University, Ottawa, Canada

In bodies of water where ice is not an annual occurrence, such as in the Southern Baltic Sea, the design of offshore wind turbines is complicated by the difficulty involved in estimating the relevant ice parameters (thickness, velocity, and strength) and their corresponding probabilities of occurrence (return periods). In this paper, the use of a Copernicus reanalysis product is evaluated for its applicability in preparing drift ice thickness distributions in the design phase of offshore wind turbines. An area surrounding the Kriegers Flak wind farm site in the Southern Baltic Sea is used as a case study. The drift ice thickness statistics of ice within the region which could potentially drift into the site were weighted according to drift directions, based on the wind direction frequency in the area. We found that between 1993-2017, drift ice at Kriegers Flak mainly occurred in 1996 with 0.1 m maximum ice thickness, in good agreement with estimations reported in the literature. Ice thickness probabilities have been created from the 1996 winter data and used as input for a fatigue damage analysis of an offshore wind turbine. The additional steps required to improve the suitability of Copernicus reanalysis data for use as input into design calculations are discussed.

1. Introduction

A rising demand for renewable energy, like offshore wind, leads to the expansion of offshore wind farms to regions of challenging environmental conditions. One such condition might be sea ice for projects planned within sub-Arctic regions such as the Baltic Sea (Tikanmäki and Heinonen, 2021). Compliant structures in ice, like lighthouses or steel channel markers, are known to experience severe vibrations due to interaction with floating ice sheets (Nord et al., 2018). A significant amount of damage may need to be considered during the overall design of an offshore wind turbine if such vibrations are expected to occur.

Few studies have assessed the fatigue load damages contributed by ice (Hendrikse et al., 2014; Hendrikse and Koot, 2019), even though multiple publications emphasized the importance of fatigue load damage caused by ice-induced vibrations (Heinonen et al., 2011; Willems and Hendrikse, 2019; Popko, 2020; Hetmanczyk et al., 2011). These analyses, when not based on deterministic values, are based on ice statistics, typically the distribution of ice thickness, ice drift speed, wind-ice misalignment angle and, rather uncommonly, ice strength. From the authors' experience the occurrence probabilities of ice thickness are especially important as the ice thickness dominates the ice failure type during an ice-structure interaction (Hendrikse and Metrikine, 2016). Whereas bending and buckling of ice results in lower loads, crushing ice and corresponding ice-structure interaction regimes are expected to induce high damages to the structure. The determination of ice occurrence probabilities can therefore be project-critical and should be based on reliable environmental data.

However, it is costly and impractical to collect accurate in-situ data on ice conditions at every location that may be of interest for offshore wind. In addition, ice measurement campaigns that are limited in duration may not give a representative view of possible ice occurrences during the lifetime of a wind farm. This is an issue in locations such as the Southern Baltic Sea, where ice is not an annual occurrence. In such cases, a method outlined by Tikanmäki and Heinonen (2021) has been used for estimating the maximum level ice and ridge ice thickness that could occur at the Kriegers Flak wind farm site in the Southern Baltic. They reviewed ice charts, reports, and atlases containing historical information on the ice occurrences at the site, along with estimating ice thicknesses from temperature records at local weather stations. They found that ice rarely occurred at the site, and for the purpose of wind turbine design, they estimated a maximum level ice thickness between 0.26 and 0.44 m (depending on the assumptions) with a 50-year return period. However, only the maximum ice thickness is reported, while a distribution is needed for estimations of fatigue damage due to ice-induced vibrations.

In this work, we assess the viability of an alternative method of estimating drift ice thickness. Our method is based on modelled data on ice conditions from large-scale air-ice-ocean dynamic models from Copernicus, the European Union's (EU) earth observation program. Within Copernicus, the Global Ocean Physics Reanalysis (GLORYS12V1) product models parameters such as sea ice thickness, velocity, and concentration (EU Copernicus Marine Service Information, 2021). Parameters are resolved at 1/12° latitude and longitude spatial resolution and given as daily means between 1993-2017 (Drévillon et al., 2021). For ease of comparison to previous work, the location around Kriegers Flak is used for this work. According to Tikanmäki and Heinonen (2021), the only occurrence of ice in the Kriegers Flak area in the period 1993-2017 was in 1996. Therefore, the winter of 1996 was focused on. Different methods of generalizing the drift ice thickness distribution are studied, by extending the area under consideration and implementing weighting methods based on wind direction frequency. Results are compared with those of Tikanmäki and Heinonen (2021).

The following research questions are formulated for this study:

1. How can the chosen Copernicus product be used to generate ice statistics suitable for use in the design of structures?
2. How does the uncertainty in ice thickness and occurrence affect fatigue damage on the offshore wind turbine used in this case study?

2. Methods

This section describes our approach to estimating the relative occurrence probabilities of ice thickness from the output of the Copernicus product GLORYS12V1.

2.1. Model drift ice thickness distribution

To create drift ice thickness distributions, the GLORYS12V1 product was accessed from the Copernicus Marine Service. In particular, the parameters ice thickness, ice velocity and ice concentration were extracted. Drift ice was considered for the analysis, i.e. ice which was estimated to have ice thickness larger than 0 m, ice drift speed larger than 0 m/s, and ice concentration above 0. This avoided the inclusion of landfast ice, which does not contribute to fatigue damage and would affect the ice thickness probability distribution if included.

2.2. Effect of drift ice distance

A central challenge was evaluating which grid cells should be considered when creating representative drift ice thickness statistics for Kriegers Flak. In this work, the Kriegers Flak area is defined as a quadrangle with corners at coordinates [54.97, 55.08] °N, [12.68, 13.1] °E, shown in Figure 1, where the quadrangle contains the two separate areas of the existing Kriegers Flak wind farm. Due to the rarity of ice in the area, simply considering the grid cells overlapping Kriegers Flak would only produce a few drift ice thickness values in this specific study. It would not be representative of the drift ice that could have occurred there given different wind conditions, or drift ice that could potentially occur there in the future. To partly address these limitations, we generalize the drift ice thickness distribution by considering the drift ice thickness in larger areas around the site, but it should be noted that we do not quantify the probability of drift.

To derive drift distances based on the estimated drift time, we use the mean wind speed and direction at the site, while assuming that the ice is primarily wind-driven. At Kriegers Flak, the mean wind speed is 7.6 m/s at 10 m above sea level (Global Wind Atlas, 2021). For free drift of thin ice, assuming a wind-induced current component is not present, the ice drift speed u can be expressed as a function of the wind speed U_a (Leppäranta, 2011, p. 187):

$$u = U_a Na = U_a \sqrt{\frac{\rho_a C_a}{\rho_w C_w}}, \quad \textbf{[1]}$$

where the Nansen number Na is expressed in terms of the density of air (ρ_a) and water (ρ_w) and drag coefficients from wind (C_a) and water (C_w). For the Baltic Sea, the free ice drift speed is often quoted to be around 0.02 - 0.03 of the wind speed (Leppäranta and Omstedt, 1990; Leppäranta and Myrberg, 2009, p. 252). If a value of 0.025 is employed, in line with previous approaches for the design of offshore wind turbines in the Southern Baltic, (Popko, 2021, p. 87), then a mean wind speed of 7.6 m/s at 10 m above sea level corresponds to an ice drift speed of 0.19 m/s. From this, drift cases can be defined based on the distance which the ice may travel over different time durations at 0.19 m/s. The drift cases used for fatigue damage calculation are shown in Table 1.

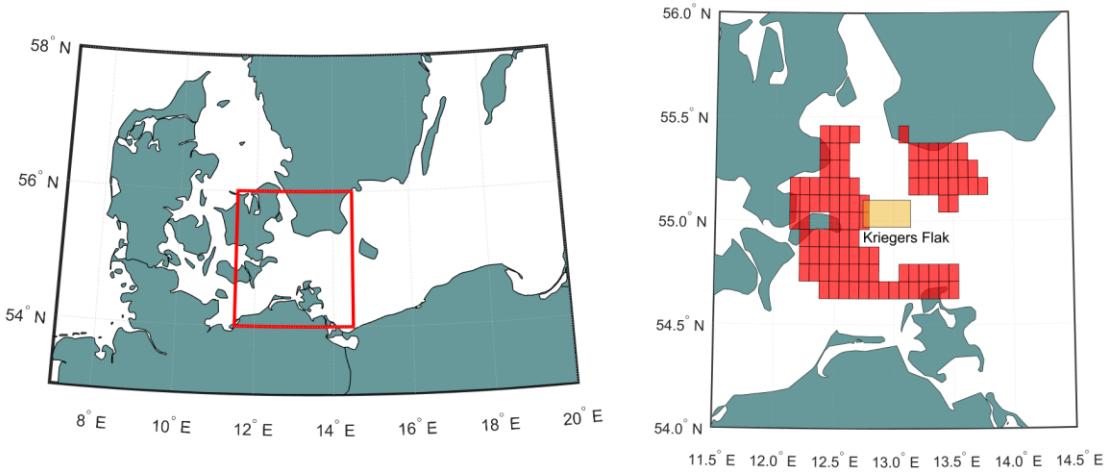

Figure 1. The left figure shows the general region under consideration marked in red. The right figure shows a zoomed-in view, with the quadrangle containing the Kriegers Flak area (marked in orange) along with all GLORYS12V1 grid cells (marked in red) where drift ice occurred within 41.04 km distance of the site, or 2.5 days of drift time at 0.19 m/s.

Table 1. Summary of the drift ice cases used for fatigue damage calculation. The cases are based on three different drift distances.

Drift case	Drift distance [km]	Drift time at 0.19 m/s
1	41.04	2.5 days
2	16.42	1 day
3	5	7.3 hours

2.3. Drift ice thickness distribution

A lower limit on considered ice thickness was introduced to emphasize crushing ice failures; ice-structure interactions involving thin ice relative to a large structure diameter (i.e., with a high aspect ratio) will typically not fail in crushing, but rather in bending due to buckling instability, which is not expected to cause significant ice-induced vibrations (Hendrikse and Metrikine, 2016). This boundary thickness has been set to 0.15 m, as full-scale observations at the Norströmsgrund lighthouse indicated that the dominant failure mode was bending rather than crushing below this threshold (Kärnä and Jochmann, 2003). As the lighthouse has a similar waterline diameter as modern offshore wind turbines, therefore keeping the aspect ratio similar for both structures, the value seems suitable for our analysis.

By counting all drift ice occurrences with thicknesses of 0.15 m or above in each grid cell, and sorting the occurrences in bins of 0.05 m, an ice thickness frequency distribution can be created. By normalizing the frequency distribution, the relative occurrence probability for drift ice with ice thickness within a bin j can be found:

$$P(\text{ice with thickness within bin } j \mid \text{ice}) = \frac{n_j}{n}, \qquad \textbf{[2]}$$

where n_j is the occurrence frequency within bin j, and n is the total number of occurrences. Thus, the relative probability distributions, found in Table 2, give an estimate of the occurrence probability of drift ice with thickness within each 0.05 m bin, but only during the days in February 1996 when there was drift ice.

2.4. Weighting of grid cells based on wind direction probability

When creating the ice thickness distributions, the ice thickness statistics are weighted based on the wind direction distribution (wind rose) at the site (Global Wind Atlas, 2021). The wind rose consists of 12 bins spanning 30° each, with magnitudes corresponding to the relative probability of winds from that direction. Drift ice in grid cells upwind from more frequent wind directions may drift into Kriegers Flak more often. Therefore, the relative magnitude of each directional bin in the wind rose was used to weight the ice thickness occurrence frequency in grid cells in that direction. That is, the weighted occurrence frequency $n_{j,w}$ is found as:

$$n_{j,w} = \sum_{i=1}^{n} w_i o_i \ , \ o_i = \begin{cases} 1, & h_i \text{ within ice thickness bin } j \\ 0, & \text{otherwise} \end{cases}, \qquad \textbf{[3]}$$

where w_i is the relative magnitude of wind direction from the grid cell containing occurrence i, and o_i is a binary counting variable. The relative weight applied to different directions is illustrated in Figure 2. A 20° turning angle between wind directions and ice drift directions was applied for the weighting calculation, as found for free drift in the Baltic Sea (Leppäranta and Omstedt, 1990).

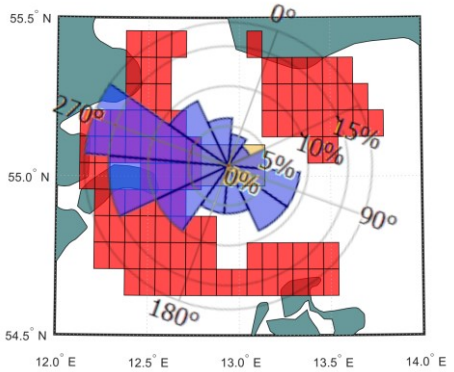

Figure 2. The wind rose at Kriegers Flak overlaid on top of the map. The relative radius of each bin corresponds to the weighting of ice thickness statistics from grid cells in that direction. The wind rose is rotated 20° degrees clockwise to simulate a wind-ice drift turning angle.

2.5. Fatigue Damage

The fatigue damage is calculated as:

$$D_{day} = (\sum M_i^m \cdot n_i)/d \ , \qquad \textbf{[4]}$$

where M_i is load level, m the Basquin (Wholer) slope, n_i the number of load cycles and d the number of occurrences in days. Here damage has been calculated for $m = 5$. The number of load cycles and load levels are based on a rainflow counting. To quantify the effect of using different ice thickness probabilities, damages for Cases 1-3, summarized in Table 1, are compared. During this case study a 14MW offshore wind turbine with a diameter of 7.5 m at mean sea level (MSL) was implemented during fatigue load analysis.

3. Results

Figure 3a) shows the number of all drift ice occurrences per GLORYS12V1 grid cell in the largest area that is considered. Because the temporal resolution is 24 hours, a drift ice occurrence in a grid cell equals a day of drift ice. There were 19 unique days where drift ice was predicted to occur in at least one grid cell, all in February 1996. In general, grid cells close to shore contain the largest number of drift ice days, particularly in the Danish bays Faxe Bugt

and Hjelm Bugt. The grid cells that partly overlap with Kriegers Flak contain 3 drift ice days, while the closest grid cell at the western edge contains 8 drift ice days. Figure 3b) shows an overview of the maximum drift ice thickness that occurred within each grid cell. Inside Kriegers Flak, there were no ice thickness occurrences above 0.15 m, the thickest was 0.10 m. Ice thicker than 0.15 m occurred in neighboring grid cells, with one of them containing ice above 0.4 m.

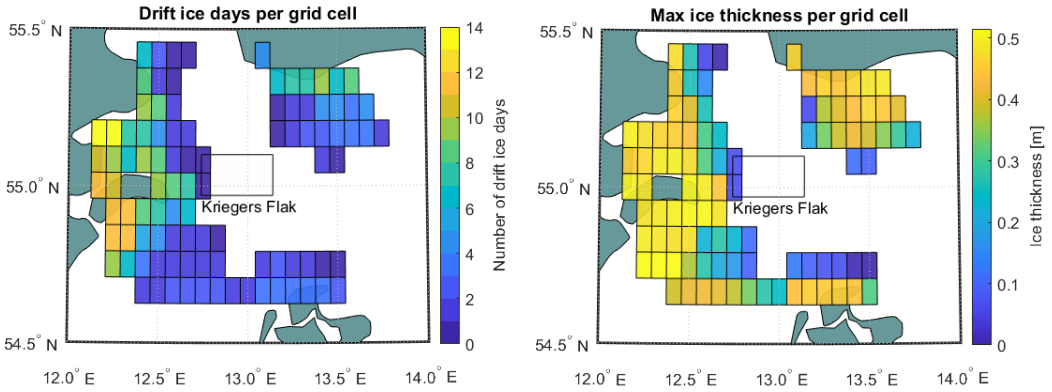

(a) (b)

Figure 3. Heatmaps showing: (a) the number of all drift ice occurrences, or drift ice days, per grid cell, and (b) the maximum ice thickness per grid cell within 41.04 km from Kriegers Flak.

3.1. Effect of considered distance

Figure 4 shows how the number of ice days and the ice thickness statistics depends on the included area around Kriegers Flak. The number of ice days with ice thickness larger than 0.15 m increases in a stepwise fashion with distance from Kriegers Flak, as more grid cells further towards land are included. The boxplot in Figure 4 shows how the median ice thickness stays quite stable when considering drift distances above 15 km, albeit with a slight increasing trend. The ice thickness distributions narrow around the median for larger distances, shifting the probability density to thicker ice as a greater number of data points and more grid cells close to land are included.

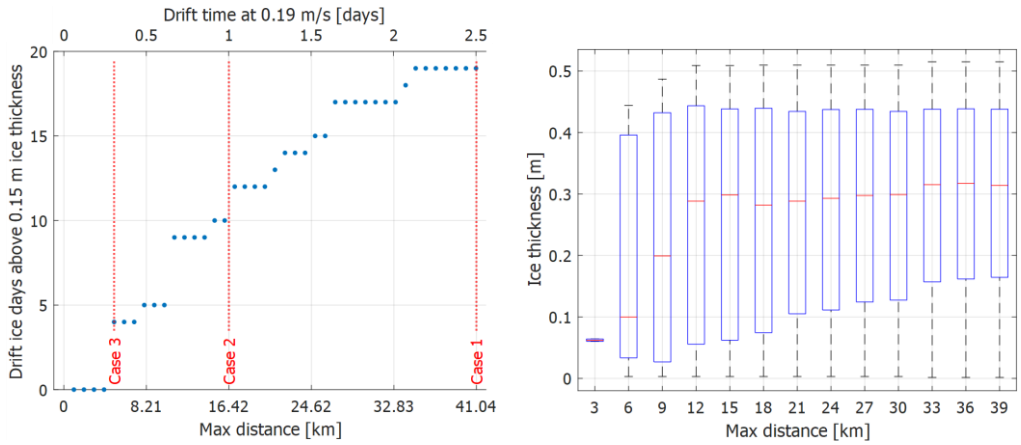

Figure 4. Left: Unique drift ice days with drift ice thickness greater than 0.15 m as the max distance from Kriegers Flak that is considered is increased. Equivalent drift times for drift speeds of 0.19 m/s are provided. Right: Boxplot of ice thickness values depending on max distance from Kriegers Flak. In the boxplot, the red, horizontal line gives the median, the box spans the interquartile range, and the whiskers indicate the most extreme values.

3.2. Fatigue damage calculation

The different ice thickness occurrence probabilities (Table 2) have been used as input for a fatigue analysis for an offshore wind turbine on monopile foundation in BHawC, an in-house aeroelastic software used by Siemens Gamesa Renewable Energy. As a reference, ice thickness occurrence probabilities as used for the Danish Kriegers Flak (DKF) project has been included as well. The ice occurrence probabilities of this project have been provided by Vattenfall. To isolate the effect of variation in ice thickness occurrence probability, other distributions and deterministic values have been kept constant as given by the DKF reference case. The simulated fatigue damage is presented in Figure 5, which shows the daily fatigue damage from the ice as a fraction of the daily fatigue damage from waves over the structural height. Thus, we here also introduce a fatigue damage related to waves. As the structural dynamics of the considered structure is non-linear, the set of wave parameters implemented in the fatigue assessment needs to represent the theoretical fatigue damage for the design lifetime and location. Therefore, a whole envelope of significant wave heights and wave periods have been applied. This envelope is representative for waves in the Southern North Sea, which are believed to result in damages in the same order of magnitude as for waves in the Southern Baltic Sea.

The results show that almost no difference between Cases 1-3 exists once the damage is normalized per day. Of course, Case 1 would result in a damage almost twice as high as Case 2, due to the increased number of occurrences. Further, the ice loading is dominating the fatigue damage per day only for structural cross sections close to tower top when this specific turbine and support structure is considered.

Table 2. Drift cases, their corresponding ice thickness probabilities, and number of occurrence days. A reference case, based on probabilities used in the design of a real wind farm, is introduced to compare to our results. Also, the number of wave occurrences are listed.

Drift case	Ice thickness [cm]	Ice thickness probabilities [-]	Number of occurrences d [days]
1	15, 20, 25, 30	0.07, 0.09, 0.14, 0.71	19
2	15, 20, 25, 30	0.08, 0.05, 0.14, 0.73	10
3	15, 20, 25, 30	0.00, 0.11, 0.22, 0.67	4
ref	15, 20, 25, 30	0.13, 0.24, 0.21, 0.42	8.9
waves	-	-	9131.25

The comparison between damage calculated for Cases 1-3 to the reference case shows that only minor differences are present. However, the fatigue damage is dominated by the number of days with ice and not by the weighting of ice thicknesses. Concentrating on the number of occurrences, the comparison to the reference case matches well with Case 2.

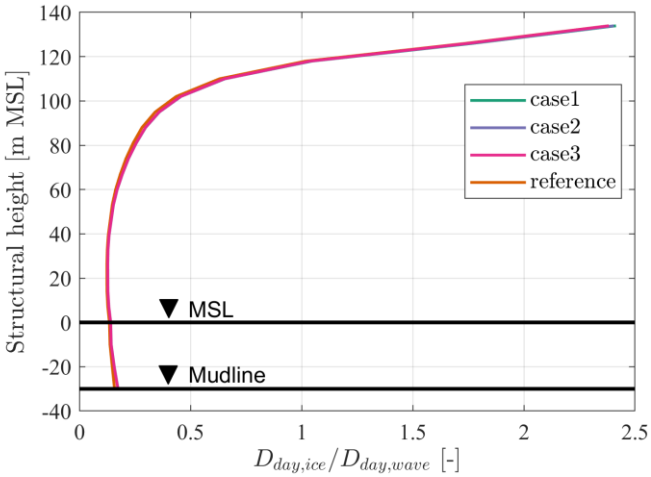

Figure 5. The fatigue damage provided by a single day of ice is normalized by the fatigue damage of a single day of waves and wind on the x-axis. The normalized value is shown over structural height of the turbine.

4. Discussion

4.1. Boundary conditions (travel distance)

This study considered different approaches to arrive at ice occurrence probabilities, such as varying the travel distance. The resulting ice thickness distribution is sensitive to the distance limiting the considered cells implemented in GLORYS12V1, shown in Figure 4. Increasing the distance means increasing the number of ice days and maximum ice thickness, as more shallow and sheltered areas, such as the Faxe Bugt and eventually Præstø Fjord, are included. The increased ice severity in these areas seen from the model is also reflected in ice atlases for the area (Schmelzer et al., 2012). Ice drift from these areas to Kriegers Flak could be unlikely for several reasons, including physical distance, obstacles in the case of sheltered areas, possible interaction with landfast ice, and possibly smaller driving forces. Using long drift distances that include areas close to land is not likely to give ice thickness representative of conditions at Kriegers Flak. The choice of travel distance is thus a trade-off between representativeness and generalization of the ice conditions that could occur from drift.

4.2. Ice thickness

The maximum ice thickness found at Kriegers Flak in this work agrees relatively well with thicknesses suggested for design by Tikanmäki and Heinonen (2021). In 1996, they estimated a maximum level ice thickness of 0.12-0.15 m based on air temperatures and ice days at the site, compared to 0.10 m from the Copernicus product. However, this is in sharp contrast to occurrences of ice thicknesses above 0.4 m in grid cells adjacent to Kriegers Flak. The increased thickness could be explained by a greater probability of a larger maximum ice thickness towards land, or by ice deformation events, such as rafting or ridging, with an associated increase in maximum ice thickness. Ice thickness statistics from the Copernicus product does not discriminate between level and deformed ice, while Tikanmäki and Heinonen specifically report the level ice thickness in their analysis. Deformation events could have been caused by strong winds and fluctuations in wind directions that could break off landfast ice, cause shear zone interaction, and raft or ridge different ice layers. However, Tikanmäki and Heinonen report only new ice at the site in 1996.

As a conservative approach, the longest drift distance considered was 2.5 days, or 41.04 km at a 0.19 m/s drift speed. This distance includes the north coast of the German island of Rügen,

where the weather station Arkona is located. Tikanmäki and Heinonen (2021) found that Arkona reported more freezing degree days compared to the weather station on Møn island, which is closest to Kriegers Flak. However, the larger number of freezing degree days only resulted in a difference in estimated ice thickness of a few centimeters between the two locations. The comparative difference in maximum ice thickness outside Møn and Arkona from GLORYS12V1 is larger, as indicated by Figure 3, indicating that the difference is influenced by more factors than just the air temperature.

It should also be noted that the ice thickness is kept constant during drift. The ice growth or melting during ice drift depends basically on the air temperatures and the initial ice thickness (for ice growth), and the oceanic flux (for melting). In our case with less than 5 days of drift both growth and melting will any way be limited to a few centimeters (most probably less than 5).

As explained in section 2.3, only ice thickness above 0.15 m is included, and the possible error from implementing such a cutoff will be related to the uncertainty in the data itself. However, estimations of ice thickness uncertainty are not given in the GLORYS12V1 quality information document, and only the validation of related parameters (such as ice concentration and volume) are mentioned (Drévillon et al., 2021). Therefore, errors in the ice thickness data used for fatigue calculations due to the cutoff should not be ruled out.

4.3. Wind direction weighting

Based on the mean wind rose, and neglecting the wind fluctuations, a weighting of grid cells was introduced. The most frequent wind directions are from the west, in the direction of shallower, more sheltered areas with more severe ice conditions, which may not be representative of conditions at Kriegers Flak. If weighting methods based on wind directions are used, the local geography and presence of factors that affect the probability of drift in that direction should not be ignored.

4.4. Limitations of study due to ice infrequency

Importantly, the analysis is based on one winter only, due to the infrequency of drift ice at Kriegers Flak and limited time duration of the Copernicus product. This may limit the statistical validity of conclusions on comparisons between the Copernicus product and other literature. Attempts to generalize the ice thickness distributions by including a larger area will still be based on ice from a single year, and its distribution depends on the severity of that winter. Note that Tikanmäki and Heinonen (2021) showed that the freezing degree days (FDD) that occurred in 1996 did not indicate a particularly severe winter, compared to previous winters where ice was reported in the Kriegers Flak area. It therefore seems unlikely that the considerably thicker ice estimated close to Kriegers Flak is caused by the relative severity of the winter in question.

4.5. Further work

The viability of using the Copernicus product as input for fatigue analysis is hampered by its limited spatial and temporal resolution. Increased resolution may give a more accurate estimate of the duration where ice is present at the site. Additionally, an increased resolution should result in a more accurate ice thickness distribution. But at Kriegers Flak, the potential increase in fatigue damage from a shift in the thickness distribution was seen to be negligible compared to the number of ice days. To improve the method of using a large area as representative, more sophisticated methods should be applied to assess the likelihood that drift ice from these areas enter the site of Kriegers Flak. For example, manually excluding bays or sheltered areas, taking local currents into account, and accounting for geographical obstacles. Note that this approach

is sensitive to the definition of the Kriegers Flak area and would have to be adjusted when applied in other locations. Additionally, while this work has focused on ice thickness probabilities only, occurrences of ice drift speed and misalignment angle have not been investigated. Furthermore, correlated combinations of ice thickness, ice drift speed, and misalignment angle are needed to build a complete input for fatigue load analysis.

5. Conclusions

Offshore wind turbines in sub-Arctic regions need to be designed to withstand dynamic ice-structure interaction. Focusing on the fatigue load assessment, occurrence probabilities of ice thickness, ice drift speed, and wind-ice misalignment are required. Determination of these is complex and time-consuming as the rarity of ice events limit the accessibility and reliability of derived probabilities. Therefore, public model data from the Copernicus program has been used to derive occurrence probabilities of ice thickness for a specific site. Methods have been explored to generalize the ice thickness distribution that may occur at a location. The number of ice occurrence days obtained from the Copernicus product are close to the reference case of a real wind farm (Danish Krieger Flak). The maximum ice thickness in the Kriegers Flak area found from the Copernicus product was close to estimations in literature, but with large differences only a few kilometers away. There were challenges with statistical validity due to rarity of ice winters in the Southern Baltic compared to the time duration of the model. The resulting fatigue damage was primarily determined by the number of days with ice, and not changes in the ice thickness distribution.

Acknowledgements

The authors wish to acknowledge the support to the FATICE project from the MarTERA partners, the Research Council of Norway (RCN), German Federal Ministry of Economic Affairs and Energy (BMWi), the European Union through European Union's Horizon 2020 research and innovation programme under grant agreement No 728053-MarTERA and the support of the FATICE partners. Further, the authors thank Siemens Gamesa Renewable Energies for their support on the fatigue damage calculation. Also, we thank Vattenfall and C2Wind for their cooperation and allowance to use ice occurrence probabilities of the 'Danish Kriegers Flak' project for verification of results. Finally, we wish to thank Torodd S. Nord for valuable discussion and feedback.

References

Drévillon, M., Régnier, C., Lellouche, J.-M., Garric, G., Bricaud, C. and Hernandez, O., 2021. CMEMS-GLO-QUID-001-030, 1.5 edn., E.U. Copernicus marine service information [Online; accessed 15.12.2021]. Retrieved from: https://catalogue.marine.copernicus.eu/documents/QUID/CMEMS-GLO-QUID-001-030.pdf

EU Copernicus Marine Service Information, 2021. GLOBAL_REANALYSIS_PHYS_001_030. In: C.M.E.M. Service. [Online; accessed 25.11.2019]. Retrieved from: https://resources.marine.copernicus.eu/product-detail/GLOBAL_REANALYSIS_PHY_001_030/

Global Wind Atlas, 2021. Data obtained from the Global Wind Atlas 3.0, a free, web-based application developed, owned and operated by the Technical University of Denmark (DTU). The Global Wind Atlas 3.0 is released in partnership with the World Bank Group, utilizing data provided by Vortex, using funding provided by the Energy Sector Management Assistance Program (ESMAP). For additional information: https://globalwindatlas.info. [Online; accessed 25.11.2021].

Heinonen, J., Hetmanczyk, S. and Strobel, M., 2011. Introduction of ice loads in overall simulation of offshore wind turbines. In Proc. 21st International Conference on Port and Ocean engineering under Arctic Conditions, Montréal, Canada.

Hendrikse, H. and Koot, J., 2019. Consideration of ice drift in determining the contribution of ice-induced vibrations to structural fatigue. In Proc. 25th International Conference on Port and Ocean engineering under Arctic Conditions, Delft, The Netherlands.

Hendrikse, H. and Metrikine, A., 2016. Ice-induced vibrations and ice buckling. Cold Regions Science and Technology, 131, pp.129-141. https://doi.org/10.1016/j.coldregions.2016.09.009.

Hendrikse, H., Renting, F.W. and Metrikine, A.V., 2014. Analysis of the fatigue life of offshore wind turbine generators under combined ice-and aerodynamic loading. In International Conference on Offshore Mechanics and Arctic Engineering, Vol 10. https://doi.org/10.1115/OMAE2014-23884.

Hetmanczyk, S., Strobel, M. and Heinonen, J., 2011. Dynamic ice load model in overall simulation of offshore wind turbines. In The Twenty-first International Offshore and Polar Engineering Conference. OnePetro.

Kärnä, T. and Jochmann, P., 2003. Field observations on ice failure modes. In Proc. 17th International Conference on Port and Ocean engineering under Arctic Conditions, Trondheim, Norway.

Leppäranta, M. and Omstedt, A., 1990. Dynamic coupling of sea ice and water for an ice field with free boundaries. *Tellus A: Dynamic Meteorology and Oceanography*, *42*(4), pp.482-495.

Leppäranta, M. and Myrberg, K., 2009. *Physical oceanography of the Baltic Sea*. Springer Science & Business Media.

Leppäranta, M., 2011. *The drift of sea ice.* Springer Science & Business Media.

Nord, T.S., Samardžija, I., Hendrikse, H., Bjerkås, M., Høyland, K.V. and Li, H., 2018. Ice-induced vibrations of the Norströmsgrund lighthouse. Cold Regions Science and Technology, 155, pp.237-251.

Popko, W., 2020. *Impact of sea ice loads on global dynamics of offshore wind turbines*. Fraunhofer Verlag.

Schmelzer, N., Holfort, J., Sztobryn, M., and Przygrodzki, P., 2012. *Climatological Ice Atlas for the western and southern Baltic Sea (1961–2010)* (N. Schmelzer & J. Holfort, Eds.) (No. BSH-Nr. 2338). Hamburg und Rostock: Bundesamt für Seeschifffahrt und Hydrographie.

Tikanmäki, M. and Heinonen, J., 2021. Estimating extreme level ice and ridge thickness for offshore wind turbine design: Case study Kriegers Flak. *Wind Energy.* 2021;1-21.

Willems, T. and Hendrikse, H., 2019. Coupled simulation of ice-structure interaction of offshore wind turbines in BHawC using VANILLA. In Proc. of the 25th International Conference on Port and Ocean engineering under Arctic Conditions, Delft, The Netherlands.